Int. J. Electrochem. Sci., 11 **(2016)** 9424 – 9437, doi: 10.20964/2016.11.44

International Journal of
ELECTROCHEMICAL
SCIENCE
www.electrochemsci.org

Hot Corrosion Resistance of Al_2O_3 Coating Produced by Thermal Spray

W. Aperador[1,*], *J. Bautista-Ruiz*[2], *E. Delgado*[1]

[1] School of Engineering, Universidad Militar Nueva Granada, Bogotá-Colombia
[2] Universidad Francisco de Paula Santander, San José de Cúcuta, Colombia
[*]E-mail: g.ing.materiales@gmail.com

Received: 12 August 2016 / *Accepted:* 17 September 2016 / *Published:* 10 October 2016

In this paper the corrosion rates of the aluminum oxide (Al_2O_3) coatings were determined, obtained through technical produced by thermal spray, using as substrate 316. The coatings were studied by potentiodynamic polarization curves Tafel and Electrochemical Impedance Spectroscopy (EIS), in an exposure time of 150 hours and three temperatures of evaluation 600 ° C, 650 ° C and 700 ° C. Subsequently the samples were cooled to room temperature to avoid the thermal shocks. The methods used X-ray diffraction and electron microscopy applied to define surface showing the attack of the molten salt. It was found increased corrosion rate as the test temperature rises. The values of the polarization resistance are greater than the substrate.

Keywords: thermal spray, Hot corrosion, molten salts, aluminum oxide.

1. INTRODUCTION

The Thermal spray is a technique of projecting droplets of molten material for coating surfaces of parts. Droplets of molten material or plastic state are accelerated in a gas jet projecting against the surface to be coated [1-3]. On the impact, fine particles in sheet form adhere to the surface, overlap and interlock to solidify [4].

The main advantage of Thermal spray processes is the variety of materials that can melt (undecomposed) to be applied as coatings [5]. Another advantage is the versatility of thermal spray processes to apply coatings to substrates without heating significantly [6]. Thus, materials with high melting temperatures can be applied to parts machined and heat treated without changing its properties. In contrast, a disadvantage is the impossibility of applying the coating to places where the torch which the material melts not accomplish [7].

The applications of thermal spray processes are extremely varied. However, their increased use categories are to improvement of corrosion resistance and wear properties of the surfaces. Other applications include use in dimensional restoration, as thermal barriers, thermal conductors, electrical conductors or resistors, for electromagnetic shields and improve or delay radiation [8]. Indeed, they are used in the aerospace, automotive, agricultural, mining, primary metals, paper, production of oil and gas, in addition to the biomedical, chemical and plastics sectors [9-10].

Thermal spray processes can deposit sprayed on any surface, especially metal materials. These materials are heated to a plastic state by combustion processes or arc, which are accelerated toward the workpiece to be coated in the form of tiny droplets hitting the surface, compacting and forming thin films that are joined [11-12]. Importantly, the temperature of the part to which is applied the coating must remain below 200 ° C, this allows preventing structural changes or metallurgical the material composing the part to be coated.

The quality of the coatings depends on certain factors such as surface adhesion to the substrate-coating interface and the degree of porosity of the film due to the cohesion of the particles that make it up [13]. In Thermal spray, has considerable influence on the adhesion of the variable coating as the impact velocity of the particles of material to be deposited on the substrate, the size, the temperature at which melt the particles, the surface temperature as the substrate roughness [14].

The high temperature corrosion commonly occurs in boilers and furnaces in most cases by the combustion of coal causing a chemical process, where most steels have its metal surface in combustion ashes whose composition consists of mixtures of sulphates and chlorides, generating problems such as decrease in heat transfer, which leads to corrosion in an accelerated manner [15-16]. This is because most low carbon alloys, have restriction because after the 650 ° C corrosion occurs at high temperatures causing a decrease in mechanical properties. The chromium alloyed steels and nickel provide good performance over 1200 ° C, due to its austenitic type structure, however after subjecting them to close to 700 ° C temperatures in prolonged periods it is presented to oxidative attack causing corrosion [17].

In this paper Al_2O_3 coatings they were obtained using the technique produced by thermal spray, which allows a coating thickness of about 50 microns, the evaluation of corrosion resistance was performed with electrochemical techniques which allow to obtain values corrosion rate and polarization resistance, for steels with and without coatings subjected to 600 ° C, 650 ° C and 700 ° C , immersed in corrosive salts, a relationship between the temperature values and the coatings obtained is generated.

2. EXPERIMENTAL PROCEDURE

The method of thermal spray coating is used for plasma arc because this is the one that generates the highest temperatures. Besides, the particle velocities are greater than the thermal spray processes flame which makes high-density coatings and adhesion are achieved in which the content of oxides is low because of the use of inert gas. For the generation of plasma in this technique he was passed argon, through an arc from gun which heats the gas and ionization is generated forming a bright

flame. The material used is aluminum oxide supplied into the plasma powder which is melted and projected to the workpiece by the plasma jet at high speed free. Temperatures used were 2300 °C. The power levels employed by this technique Plasma Guns was 50 kW. Speeds powder used during deposition was 330 m/s. These variables produce coatings with higher densities, adhesion and internal stress. Ranges coatings thicknesses are about 0.05 mm.

The electrochemical cell consists of an array of 3 electrodes: the working electrode, the reference electrode and auxiliary electrode. The working electrode was welded to a platinum wire which served as an electrical conductor, this wire also was placed inside a ceramic tube of mullite industrial grade so only the specimen was exposed to the corrosive environment. The reference electrode and counter electrode were built with high purity platinum wire, which were introduced into a mullite tube resistant to high temperatures; the hollow parts between the specimen and the ceramic tube were sealed with refractory cement as the spaces of the other electrodes.

The corrosive agent used in the test is composed of a mixture of pentoxide vanadium V_2O_5 and sodium sulfate Na_2SO_4 analytic grade to concentrations (percentage of weigh) 50:50, the mixture was macerated during 45 minutes in mortar for homogenize, then were placed in a porcelain crucible of 30 g that was inserted inside on a vertical furnace. The electrochemical cell was placed in the furnace and the heating starts from room temperature to 600°C, 650°C and 700 °C needed to perform the electrochemical tests (figure 1). The internal temperature was monitored by mean of a type k thermocouple connected to a temperature controller. To resemble a boiler environment was determined the use of a mixture of oxidizing gas 99%O_2-1%SO_2.

For measurements of EIS, the sample was placed in an induction furnace and heated from room temperature to 600 ° C, 650 ° C and 700 ° C and then this temperature is maintained for 45 minutes in an air atmosphere, while the electrochemical measurements were taken. Finally, the sample was cooled down until the ambient temperature to avoid thermal shock. The experimental assembly for electrochemical analysis is shown in Fig. 1. Electrochemical measurements were performed with a Gamry potentiostat instrument PCI4G750 adapted to a frequency response analyzer. Electrochemical Impedance Spectroscopy (EIS) and Tafel polarization curves were obtained in situ at three different temperatures using a cell with a working electrode and an exposed of 1 cm^2 area, a counter electrode platinum wire (EC), and a reference electrode platinum wire (RE). To simulate hot corrosion process, a mixture of vanadium pentoxide (V_2O_5) and sodium powders (Na_2SO_4) sulfate in a 55:45 and 50:50 (wt%) relative concentration 30 g/cm^2, they were used as a molten salt.

Nyquits plots were recorded using amplitude of the sinusoidal signal of 10mV applied to the working (sample) and reference electrodes, in a frequency range of 0.1 Hz to 300 kHz. Tafel polarization curves were obtained at a scan rate of 1 mV / s in a voltage range between -0.25 to 0.25 V vs Eref, defined with respect to open circuit potential (OCP).

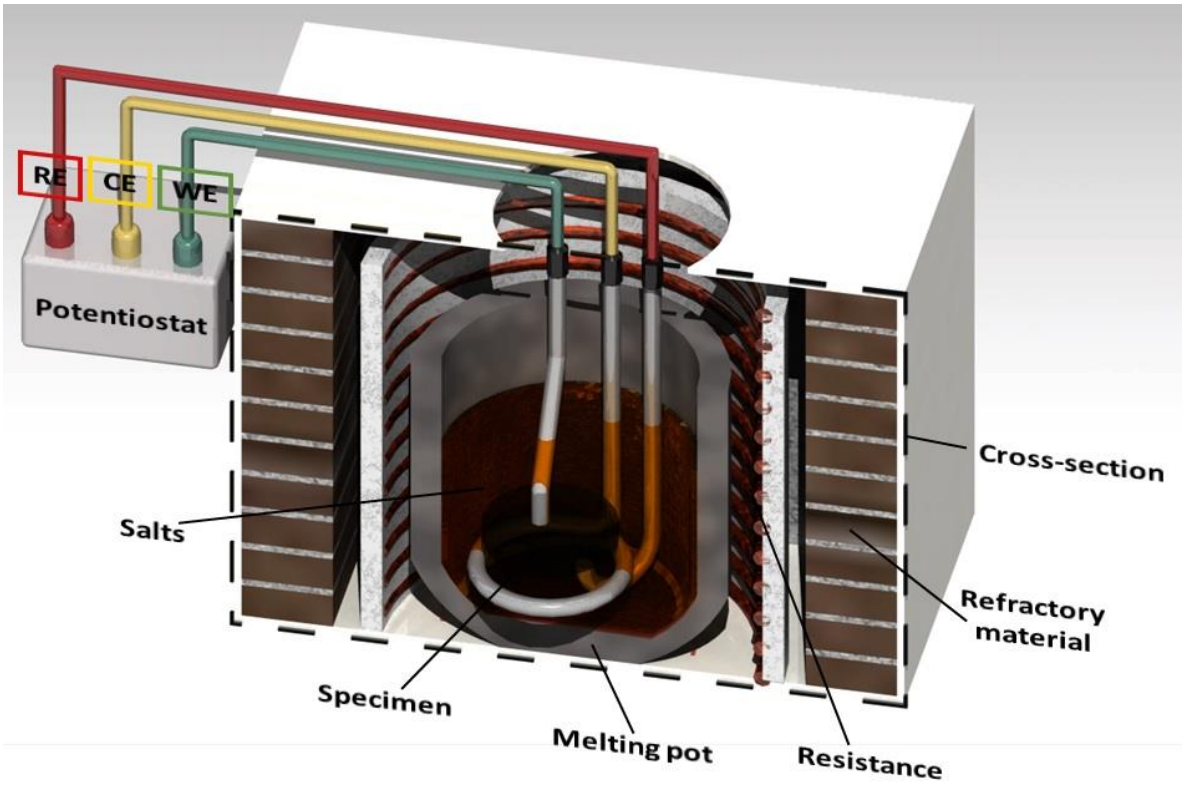

Figure 1. Oven that was used for the electrochemical tests at high temperatures.

3. RESULTS

3.1. Coating microstructures.

The thermal spray process provides good mass transfer and heat plus a uniform temperature, and a high degree of mixing of the gases with Al_2O_3 particles, allowing a high degree of reaction of all the active species. The use of the above properties allows reducing operation times against other processes [18]. Deposited on the substrate particles called splats in this case which solidify and adhere to one another to form a continuous layer [19]. Splats are created when molten and accelerated particles impact on steel AISI 316. The molten droplets are generally spherical arriving, and on impact with the substrate surface and fill expand the underlying interstices [20]. Drops become flattened disc-shaped structures. The thermal spray processes are characterized by rapid solidification. As individual particles impacting on the substrate, the heat is released faster [21]. The solidification rates are around about 110 ° C / s. In Figure 2, the grain size is about 4 μm this prevented aluminum oxide reach their equilibrium phases, thus resulting in anisotropic properties in the coating is observed, since the coating by thermal spraying consist many layers of thin particles, overlapping, this is due to the high particle velocity, because the denser and better adhesion coatings were obtained, The extent of oxidation that occurs during the process depends on the material being laid, the deposition method and the specific deposition process.

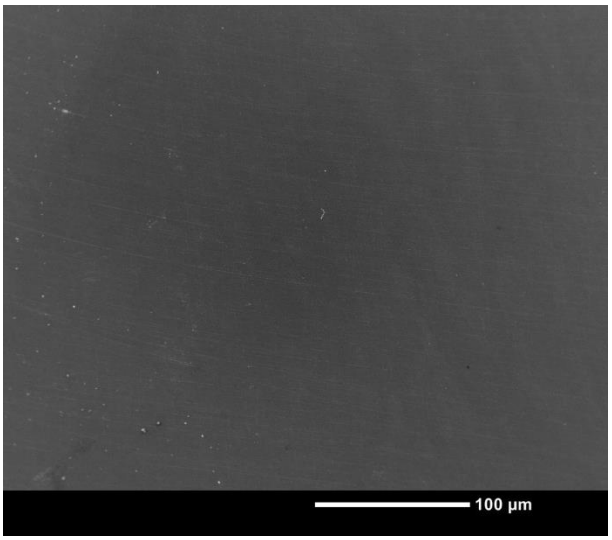

Figure 2. Micrograph of the deposited coating on steel 316 without exposure to hot corrosion.

3.2. Corrosion

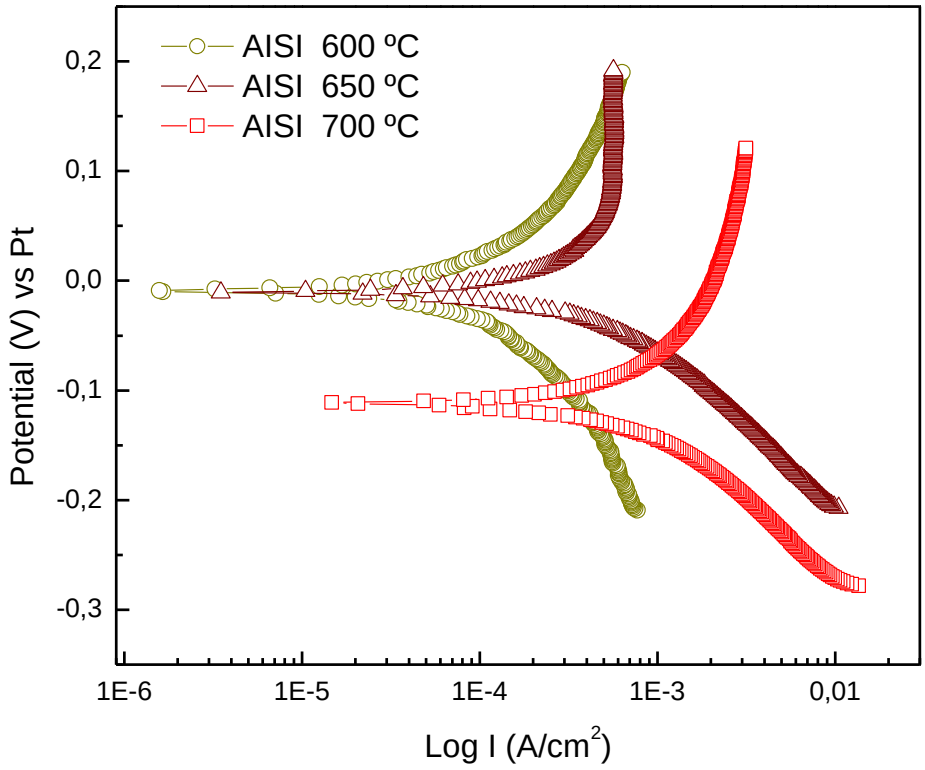

Figure 3. Polarization curves steels used as substrates and tested for 150 hours at different temperatures, immersed in corrosive salts of a mixture of pentoxide vanadium V_2O_5 and sodium sulfate Na_2SO_4, atmospheres formed by gas mixtures 99%O_2-1%SO_2.

In figures 3 the polarization curves for the steel and the coating evaluated between 600 ° C and 700 ° C are observed, for the purpose of determining the different steps that are generated in this type of system, start, acceleration and propagation [22]. Regarding the steel exposed to hot corrosion polarization curves which generally frame system general corrosion are obtained where the three curves show a cathodic region where the metal dissolution predominates in which the current rise the increasing the potential. Stainless steel is characterized by generating a passivating layer due to the reaction of its components especially chromium with oxygen, however temperatures evaluated is not possible to observe the generation of the passivating layer [23]. Relative to the trend corrosion potential is obtained that as the temperature increases in the steel test potential shifts to the negative direction, according area where the electrochemical behavior is lessened, decreasing the protective effect on each system as there rising temperatures. With respect to the corrosion rate shown in Table 1, it may indicate that because it has lost the protection which oxidation starts at 600 ° C is generated and is spread to 700 ° C, as boost more than 10 times the rate of degradation.

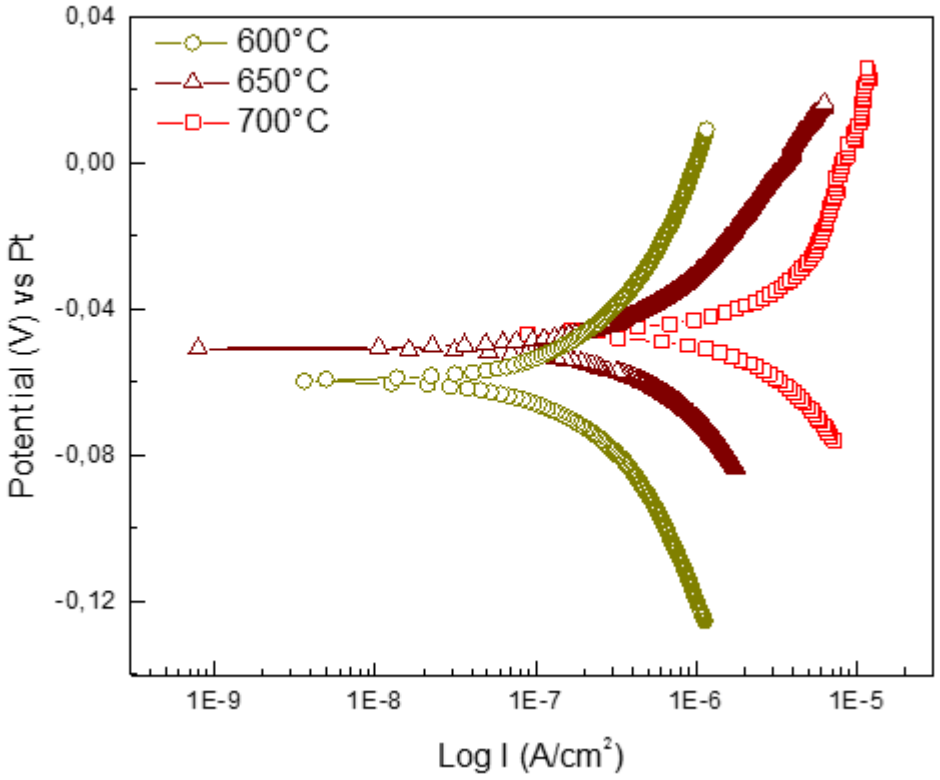

Figure 4. Polarization curves of Al_2O_3 coatings in which the gradual boost in the current density as the test temperature increases is observed, the coatings are immersed in corrosive salts of a mixture of pentoxide vanadium V_2O_5 and sodium sulfate Na_2SO_4, atmospheres formed by gas mixtures 99%O_2-1%SO_2.

Figure 4 shows the protective effect of the coatings of Al_2O_3 is observed wherein the polarization curves are similar to those obtained for the substrate behavior, because the area of the anodic showing greater dissolution with increasing temperature, with respect to potential corrosion

trend it is not established since the values generated are similar [24]. With respect to the corrosion current, a decrease is observed when compared with substrates evaluated at the same temperatures, this is because the coating generated a specific protection as cathodic corrosion reaction is related to melt blends and coating where the damage is minimal, delays the onset of corrosion for temperatures 600 and 650 ° C (Table 1), the enhance in speed is generated at 700 ° C and is due to increased diffusion, because the vanadium pentoxide is solid at this temperature the percentage of this compound in the mixture is 50%, so this effect is associated with this salt, another element present in the mixture which generates an boost in the corrosion rate going from 600ºC to 650 ° C is due to the presence of sodium, due to this compound has a lower melting point [25-26].

Table 1. Electrochemical parameters determined from curves potentiodynamic calculated from tests at the three temperatures for steels used as substrates and coatings of aluminum oxide, immersed in corrosive salts of a mixture of pentoxide vanadium V_2O_5 and sodium sulfate Na_2SO_4, atmospheres formed by gas mixtures 99%O_2-1%SO_2.

	AISI 316			Al_2O_3		
	700°C	650°C	600°C	700°C	650°C	600°C
Tafel slopes βa mV/dec	-87.49	-102.18	-37.43	-51.49	-33.4	-79.17
Tafel slopes β_c mV/dec	110.84	180.09	42.04	62.95	64.22	114.87
Corrosion potential mV	-109.01	-11.81	-7.94	-45.93	-50.95	-60.04
Corrosion current μA/cm^2	1068	425	92.8	2.08	0.3416	0.110
Corrosion rate/ mpy	375.94	149.60	32.66	0.73	0.12	0.038

In Figure 5, diagrams impedances seen by Nyquist for steels used as substrates, stages in this scheme presented in hot corrosion is clearly observed 600 ° C incubation process where the greatest value is obtained impedance is observed then 650 ° C the acceleration of the process is determined by the decrease in the total system impedance, as half the value found at 600 ° C is reduced; for 700 ° C is spread since it is the system where lower impedance value is recorded, the shapes of the curves indicate the performance of the protective layer, the lower the temperature value is generated two semicircles that are related to the formation of corrosion inhibiting products, this is due to the

compounds of nickel and chromium [28]. The higher the temperature the protective layer is destroyed and sulfidation is generated by diffusion of sulfur into the steel so that the corrosion rate increased by more than 10 times [29].

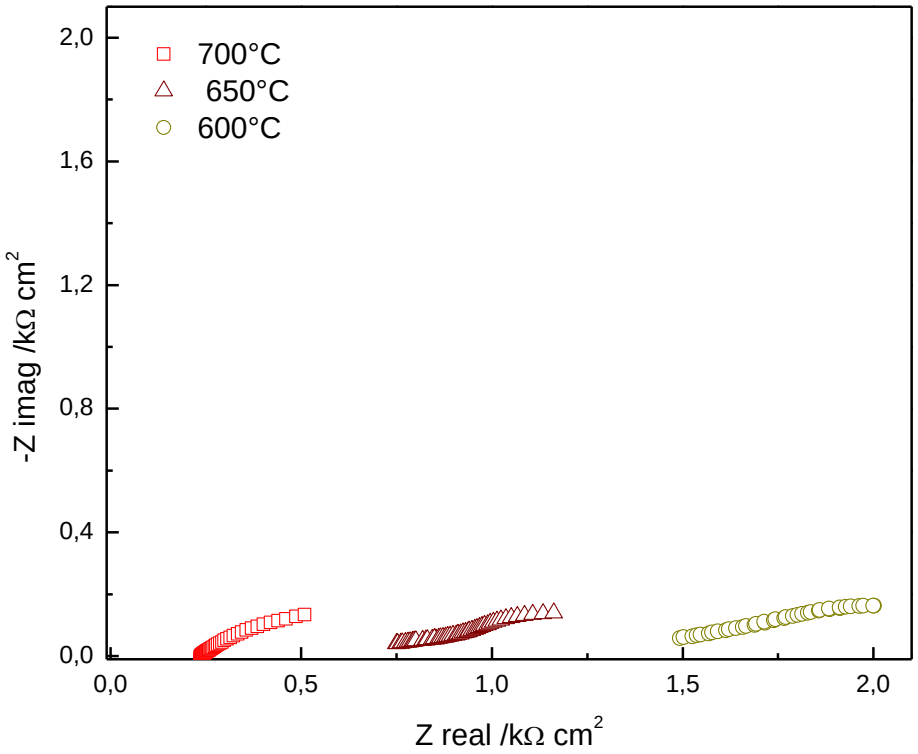

Figure 5. Nyquist diagrams corresponding to 316l steel, evaluated at three different temperatures for 150 hours, immersed in corrosive salts of a mixture of pentoxide vanadium V_2O_5 and sodium sulfate Na_2SO_4, atmospheres formed by gas mixtures 99%O_2-1%SO_2.

In Figure 6, the capacitive resistive behavior of the coatings is determined, the variation is obtained is due to the conductivity of the electrolyte improve on with temperature. Therefore microstructure constituents suffer a variation this is observed by changing the porosity [30]. The total impedance of the system evaluated at 600 ° C, has the highest value generated due to a suitable resistance value between the solution and the coating additionally a high value of the polarization resistance of the interface coating / metal, addition capacitance values generate an intact layer, that is corresponding to that obtained in the characterization by scanning electron microscopy [31]. Nyquist plots corresponding to 650 ° C and 700 ° C gradually decreased as it is noted that obtained in the polarization curves; wherein the corrosion rate increases with temperature, this is associated with the melting point of the mixture of corrosive salts entering the structure more easily due to the volumetric expansion generating a path for interconnecting pores and thus the total impedance of the coating is decreased.

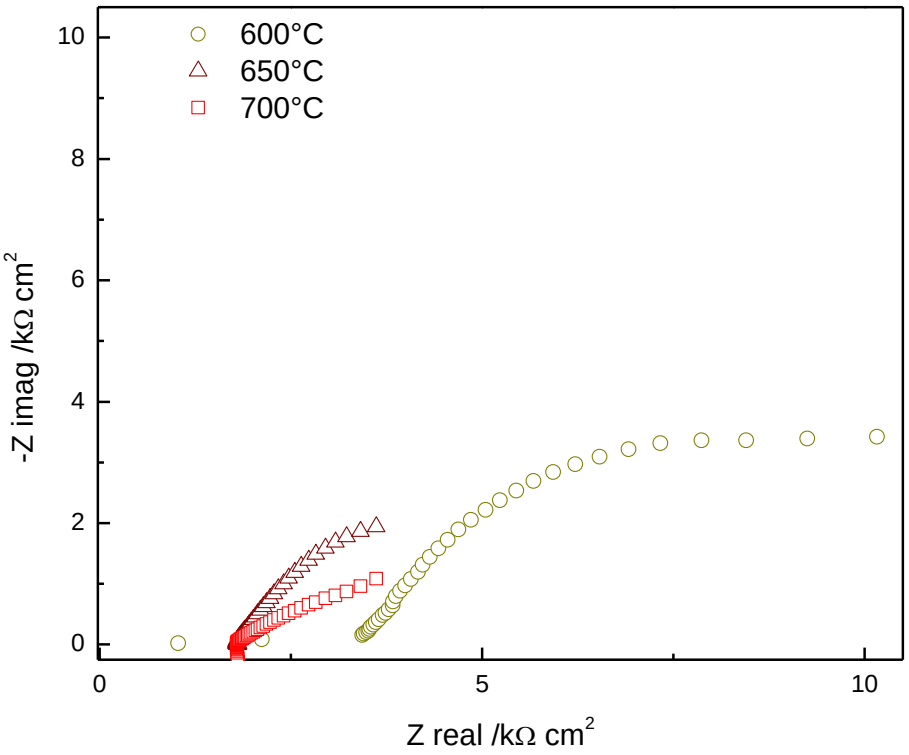

Figure 6. Diagram impedances coatings aluminum oxides evaluated at three different temperatures, where they evidence the loss of impedance at the same time that the temperature increases, the coatings are immersed in corrosive salts of a mixture of pentoxide vanadium V_2O_5 and sodium sulfate Na_2SO_4, atmospheres formed by gas mixtures 99%O_2-1%SO_2.

3.3. Microstructural analysis after the hot corrosion process

In Figure 7, micrographs of the coatings are observed after cooling in the three temperatures is a fine network observable microcracks perpendicular to the plane of the layers. These microcracks are formed by the stresses produced by the restriction of thermal contraction of the coatings and the contact with salts and subsequent cooling to corrosive attack [32]. Tensions are observed for temperatures of 650 °C and 700 °C, because it volumetrically boost material and enable deformation thereof under thermal stresses, this improve the tolerance of deformation and fatigue resistance. As the temperature enhance a surface with increased wear on the coating, where detachment of the protective layer is evidence to 600 ° C is observed a composite molten salt surface be seen, which they are responsible for significant corrosion, in the figure 7a is evidence protection coating where the area is less affected because is in an initiation stage during which the corrosion rate is much slower.

The system used is corrosion attack accelerated corrosion at high temperature (600 ° C to 700 ° C), the flow model salt is a mixture of vanadium pentoxide (V_2O_5) and sodium Na_2SO_4 sulfate, in a mixture of equal proportions. Vanadium (V), sodium (Na) and sulfur (S) are common impurities of

combustion [33]. During the combustion process, the vanadium is oxidized to form different oxides, the most representative V_2O_5, while sulfur is involved with sodium and creates sulphates, this salt is an electrolyte ionic conductor, therefore hot corrosion is electrochemical in nature, and involves flow of protective metal oxides also as solutes acids or molten salt.

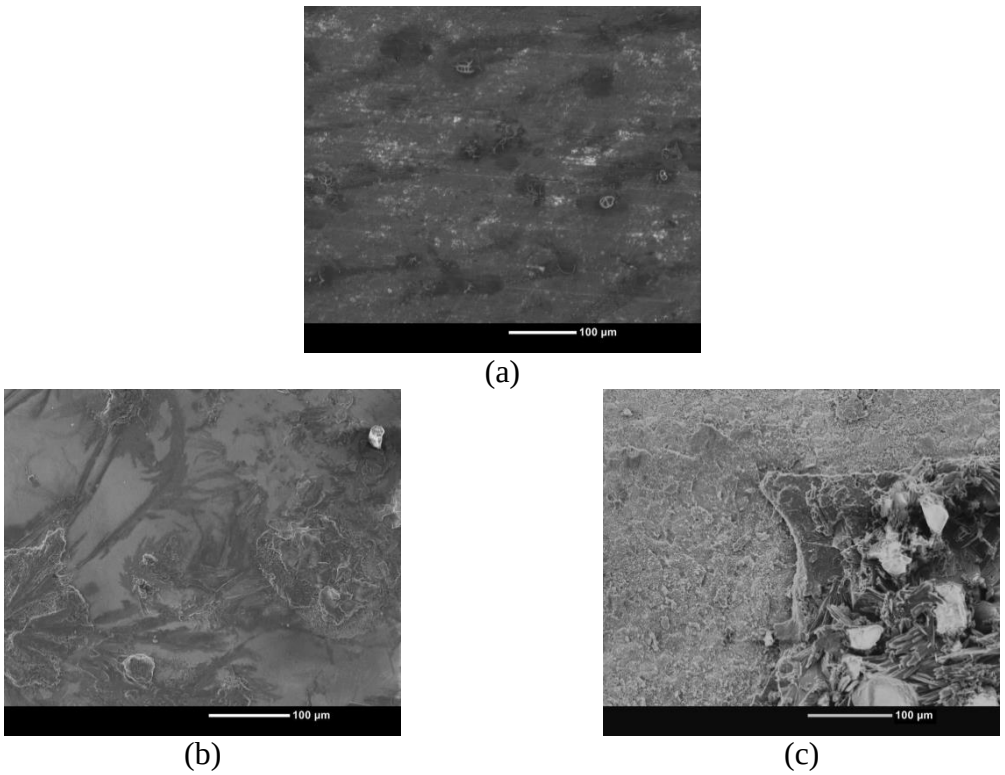

(a) (b) (c)

Figure 7. Micrographs corresponding to surfaces evaluated after exposure to high temperature corrosion, a) 600 ° C surface with less damage microstructure b) worn surface be seen due to dissolved salts on the coatings, c) damage microstructural effect accelerated corrosion at high temperatures.

3.4. X-ray diffraction

In Figure 8 the main products of the reaction between the metal and molten salt film are shown oxides oxovanadium sulfate, bannermanita ($Na_{0.7}6O_{15}V_6$ which crystallizes in the monoclinic system) and sodium sulfate, the solubility of these oxides in molten defines corrosion resistance. The specters of XRD coincide for the three tests performed at different temperatures, indicating that only one incubation step was obtained, because no contributions to the coating or substrate components in the components found in the XRD spectrum are corrosive salts at 670 ° C are liquid, so the effect is greater for temperatures approaching 700 ° C, however as can be seen in the micrographs the protective layer is not compromised a number of pores 650 ° C are observed and film cracking 700 ° C, this is due to change to solid state reaction of salts leading to the generation of reaction without the formation of sulphides that are accelerating the degradation process of the coating [34].

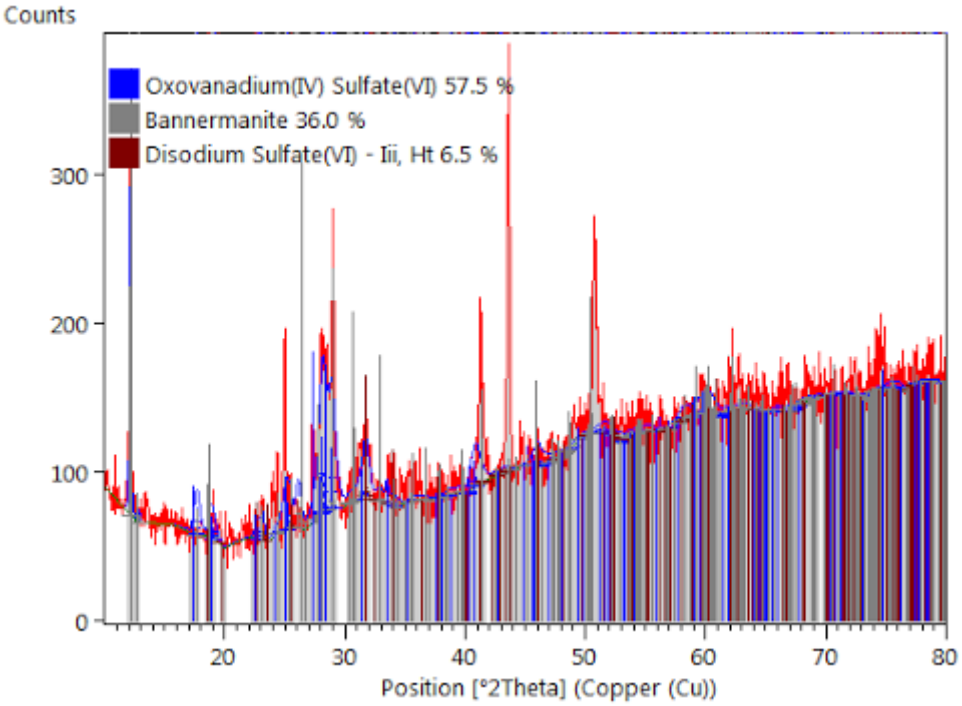

Figure 8. Corrosion products Al_2O_3 coatings evaluated at high temperatures 600 ° C, 650 ° C and 700 ° C.

3.5. Porosity factor

In Figure 9 it is observed the factor estimated porosities for coatings deposited by plasma and evaluated in the range of 600 to 700 ° C that they are among 20% and 26%. Because porosity is another important feature of the coatings that strongly influences the mechanical and durability properties. For this study the porosity can be a desirable characteristic and is generally associated with a large number of unmelted particles or re-solidified to become embedded in the coating [35]. For the calculation factor Porosity ratio polarization resistance found through the EIS technique it was used the relationship is the resistance generated by the uncoated substrate relative to that generated by the coating evaluated at each temperature, these values are represented in Table 2.

Table 2. Parameters found by electrochemical impedance spectroscopy coatings, used for the determination of porosity.

Temperature / °C	600	650	700
Polarization resistance of steel / kohms cm^2	2.82	1.55	1.11
Polarization resistance of Al_2O_3 / kohms cm^2	15.05	6.44	4.23

Porosity exposed, can interface with the environment surface to be coated, which tends to cause corrosion or the oxidation of this. The porosity can eliminate corrosion characteristics typical of the coating composition. Regarding the surface hardening or wear resistant coatings porosity decreases the hardness of the coating and contributes to poor surface finish, thereby decreasing wear resistance. The porosity in this class of coatings also leads to generation of fragments (spline) of the coating which become abrasive elements thereby increasing wear rates.

The porosity in this type of coating is generally composed of aluminum oxides, which themselves are good thermal insulators. A 18% porosity in these coatings heighten its insulating properties it said porosity also enhance the thermal shock resistance and resistance to thermal fatigue increasing the temperature raising the porosity, these results respond to the boost in the corrosion rate as temperature raise the effect is due to volumetric expansion where the links are separated generating discontinuities contributing factor to increased porosity [36].

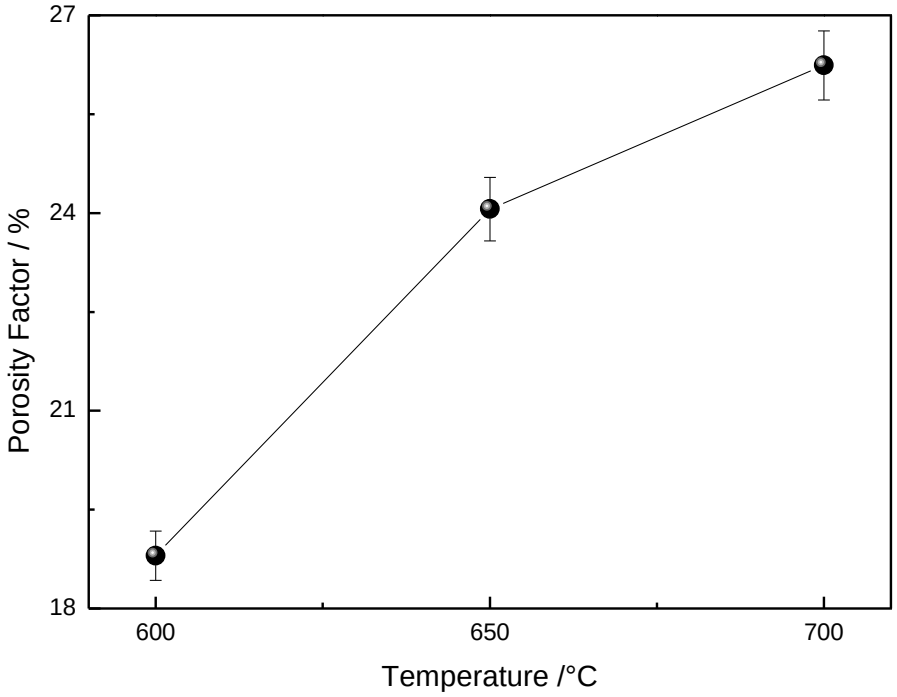

Figure 9. Porosity factor calculated from data Polarization resistance of the substrate and coating according to the temperature.

4. CONCLUSIONS

Coatings of Al_2O_3 obtained by thermal spray exhibit excellent performance in hot corrosion, due to its high volumetric density of the coating the corrosion rate decreases at high temperatures, as only the starting area is obtained unlike the steels having high speeds due to the propagation. Microcracks and a degree of porosity are beneficial, since they inhibit growth of higher cracks in the coatings.

ACKNOWLEDGEMENTS
Thanks the financial support from the Universidad Militar Nueva Granada, contract number ING-2100-2016

References

1. V. Ebrahimian, C. Habchi, *Int. J. Heat Mass Transfer*, 54, (2011) 3552.
2. R. Hays, D. Maynes, J. Crockett, *Int. J. Heat Mass Transfer*, 98 (2016) 70.
3. R.S. Volkov, G.V. Kuznetsov, J.C. Legros, P.A. Strizhak, *Int. J. Heat Mass Transfer*, 95 (2016) 184.
4. F.J. Higuera, *J. Aerosol Sci*., 91 (2016) 78.
5. B. Vajdi Hokmabad, S. Faraji, T. Ghaznavi Dizajyekan, B. Sadri, E. Esmaeilzadeh, *Int. J. Multiphase Flow*, 65 (2014) 127.
6. R. Ghafouri Azar, Z. Yang, S. Chandra, J. Mostaghimi, *Int. J. Multiphase Flow*, 26 (2005) 334.
7. F. Sánchez, A.S. Kaiser, B. Zamora, J. Ruiz, M. Lucas, *Int. J. Heat Mass Transfer*, 89 (2015) 1190.
8. M. Al Qubeissi, S.S. Sazhin, J. Turner, S. Begg, C. Crua, M.R. Heikal, *Fuel*, 159 (2015) 373.
9. G.V. Kuznetsov, P.A. Strizhak, R.S. Volkov, O.V. Vysokomornaya, *Int. J. Therm. Sci*., 108 (2016) 218.
10. A. Zacarías, M. Venegas, A. Lecuona, R. Ventas, I. Carvajal, *Exp. Therm Fluid Sci*, 68 (2015) 228.
11. A.K. Krella, A.T. Sobczyk, A. Krupa, A. Jaworek, *Mech. Mater*, 98 (2016) 120.
12. A.P. Newbery, P.S. Grant, R.A. Neiser, *Surf. Coat. Technol*, 195 (2005) 91.
13. M. Bedel, G. Reinhart, A.-A. Bogno, Ch.-A. Gandin, S. Jacomet, E. Boller, H. Nguyen-Thi, H. Henein, *Acta Mater*., 89 (2015) 234.
14. D.K. Christoulis, D.I. Pantelis, N. De Dave-Fabrègue, F. Borit, V. Guipont, M. Jeandin, *Mater. Sci. Eng.*, A, 485 (2008) 119.
15. S. Sutha, S.C. Vanithakumari, R.P. George, U. Kamachi Mudali, Baldev Raj, K.R. Ravi, *Appl. Surf. Sci*, 347 (2015) 839.
16. J.P. Hindmarsh, D.I. Wilson, M.L. Johns, *Colloids Surf*., A , 234 (2004) 129.
17. G. Castanet, F. Lemoine, *Proc. Combust. Inst*. 31 (2007) 2141.
18. A.J. Consuegro, A.S. Kaiser, B. Zamora, F. Sánchez, M. Lucas, M. Hernández, *Build. Environ*., 78 (2014) 53.
19. T. Varis, D. Bankiewicz, P. Yrjas, M. Oksa, T. Suhonen, S. Tuurna, K. Ruusuvuori, S. Holmström, *Surf. Coat. Technol*, 265 (2015) 235.
20. M. Bedel, G. Reinhart, A.-A. Bogno, Ch.-A. Gandin, S. Jacomet, E. Boller, H. Nguyen-Thi, H. Henein, *Acta Mater*., 89 (2015) 234.
21. S. Sutha, S.C. Vanithakumari, R.P. George, U. Kamachi Mudali, Baldev Raj, K.R. Ravi, *Appl. Surf. Sci*, Volume 347, 30 August 2015, Pages 839-848
22. A. Pragatheeswaran, P.V. Ananthapadmanabhan, Y. Chakravarthy, Subhankar Bhandari, Vandana Chaturvedi, Nagaraj A., K. Ramachandran, *Surf. Coat. Technol*, 265 (2015) 166.
23. D. Chaliampalias, G. Vourlias, E. Pavlidou, G. Stergioudis, S. Skolianos, K. Chrissafis, *Appl. Surf. Sci*, 255 (2008) 3104.
24. M.H. Sadafi, I. Jahn, A.B. Stilgoe, K. Hooman, *Int. J. Heat Mass Transfer*, 78 (2014) 25.
25. A.P. Newbery, T. Rayment, P.S. Grant, *Mater. Sci. Eng*., A, 383 (2004) 137.
26. B. Torres, M. Campo, M. Lieblich, J. Rams, *Surf. Coat. Technol*, 236 (2013) 274
27. M.F. Morks, C.C. Berndt, *Appl. Surf. Sci*, 256 (2010) 4322.
28. B. K. Ozcelik, C. Ergun, *Ceram. Int*., 41 (2015) 1994.
29. P. Gavendová, J. Čížek, J. Čupera, M. Hasegawa, I. Dlouhý, *Procedia Mater. Sci*, 12 (2016) 89.

30. K. Slámečka, L. Čelko, P. Skalka, J. Pokluda, K. Němec, M. Juliš, L. Klakurková, J. Švejcar, *Int. J. Fatigue*, 70 (2015) 186.
31. G. Bolelli, D. Bellucci, V. Cannillo, R. Gadow, A. Killinger, L. Lusvarghi, P. Müller, A. Sola, *Surf. Coat. Technol*, 280 (2015) 232.
32. E. Garcia, J. Mesquita-Guimarães, P. Miranzo, M.I. Osendi, *Surf. Coat. Technol*, 205 (2011) 4304.
33. M. Bastwros, G. Y. Kim, *Powder Technol*., 288 (2016) 279
34. L. Gu, X. Fan, Y. Zhao, B. Zou, Y. Wang, *Surf. Coat. Technol*, 206, (2012) 4403.
35. S. X. Hou, Z. De Liu, D. Y. Liu, B. R. Li, N. Zhang, *Mater. Sci. Eng*., A, 518 (2009) 108.
36. M.H. Sadafi, S. González Ruiz, M.R. Vetrano, I. Jahn, J. van Beeck, J.M. Buchlin, K. Hooman, *Energy Convers. Manage*, 108 (2016) 336.